Bogoliubov theory of Feshbach molecules in the BEC-BCS crossover

M. W. J. Romans,[1] and H. T. C. Stoof[1]

[1]*Institute for Theoretical Physics, University of Utrecht,*
Leuvenlaan 4, 3584 CE Utrecht, The Netherlands.
(Dated: February 4, 2008)

We present the Bogoliubov theory for the Bose-Einstein condensation of Feshbach molecules in a balanced Fermi mixture. Because the Bogoliubov theory includes (Gaussian) fluctuations, we can in this manner accurately incorporate both the two-body and many-body aspects of the BEC-BCS crossover that occurs near a Feshbach resonance. We apply the theory in particular to the very broad Feshbach resonance in atomic ^{6}Li at a magnetic field of $B_0 = 834$ G and find good agreement with experiments in that case. The BEC-BCS crossover for more narrow Feshbach resonances is also discussed.

I. INTRODUCTION

Since the achievement of Bose-Einstein condensation (BEC) in an atomic Bose gas [1, 2, 3], the field of ultracold gases has been one of the most active fields in physics. This is primarily due to the fact that these gases are very clean, accessible, and easy to manipulate. For both theorists and experimentalists, ultracold atomic gases have therefore become an important playground for the study of a diverse set of quantum phenomena, that often in other guises also appear in very different condensed-matter systems. At present also degenerate atomic Fermi gases are available [4] and have been at the center of attention in the last two years. In particular, the superfluid Bardeen-Cooper-Schrieffer (BCS) phase has been created in two-component Fermi mixtures [5, 6, 7, 8, 9, 10]. To overcome the problem of the small critical temperature, which depends in general exponentially on the interaction strength, all experiments have made use of a Feshbach resonance [11, 12, 13]. In this manner the interactions between the atoms can be strongly enhanced by an external magnetic bias field, giving rise to the BEC-BCS crossover phenomenon [14, 15, 16]. As a result of the atomic physics of the Feshbach resonance, the nature of the Cooper pairs in the BEC-BCS crossover is, however, not solely determined by the interaction strength or scattering length, but in principle also depends on the width of the Feshbach resonance. In the limit of an infinitely broad resonance, the properties of the gas can be derived from a single-channel theory that requires only the resonant scattering length as an experimental input. In general, however, a two-channel theory is needed. This is in particular true for the description of the wave function of the Cooper pairs that plays an important role in the BEC-BCS crossover as we will show in this paper.

In the crossover experiments with atomic ^{6}Li, on which we focus mostly in this paper, the atomic gas is spin polarized with respect to the electron spin of the atoms. In the event of a collision, the two atoms therefore approach each other in a triplet state, which is called the open channel. Due to the hyperfine interaction, there is a nonzero coupling to a closed singlet channel, which has a different interatomic interaction potential that, most importantly for our purposes, contains a bound molecular state. This bound molecular state we call the bare molecule from now on. Moreover, the triplet state has a magnetic moment, and the energy of the two incoming atoms can thus be tuned by a magnetic field due to the Zeeman effect. Near a Feshbach resonance, the threshold energy of the open channel is exactly tuned near a bound state of the closed channel and the nonzero coupling between the two channels causes the scattering cross section between the atoms to be resonantly enhanced, in a similar manner as in many collision experiments discovering new elementary particles in high-energy physics.

In this paper we aim at presenting a theory of the BEC-BCS crossover that includes (Gaussian) fluctuations on top of the mean-field theory. Moreover, we include the above mentioned two-channel physics of the Feshbach resonance exactly and in this way improve upon the various theories [17, 18, 19, 20, 21, 22, 23, 24, 25, 26, 27] that have also been used to discuss different aspects of the BEC-BCS crossover observed experimentally. Some consequences of our theory were previously obtained in Ref. [28]. Here we considerably expand upon that work by giving a detailed derivation of our Bogoliubov, or random-phase approximation (RPA), theory and present new results in the BEC, unitarity, and BCS limits of the theory. The main physical idea behind the theory is that the entire BEC-BCS crossover can be seen as a Bose-Einstein condensation of pairs or dressed molecules, that in the extreme BEC limit are the bare molecules, and in the BCS limit the atomic Cooper pairs. The wave function of these dressed molecules is given by the linear superposition

$$\langle \mathbf{r} | \chi_{\text{dressed}} \rangle = \sqrt{Z} \chi_{\text{m}}(\mathbf{r}) | \text{closed} \rangle + \sqrt{1-Z} \chi_{\text{aa}}(\mathbf{r}) | \text{open} \rangle, \quad (1)$$

where $\mathbf{r}$ is the interatomic distance. The parameter Z is the probability of the dressed molecule to be in the bare molecular state in the closed-channel of the Feshbach resonance. The spatial part of the bare molecular

wave function is denoted by $\chi_{\mathrm{m}}(\mathbf{r})$. The spin part of the bare molecule is equal to $|\mathrm{closed}\rangle$, in agreement with the fact that it is a bound state in the closed channel. The open channel has the spin state $|\mathrm{open}\rangle$ and the spatial part of the wave function in this channel is $\chi_{\mathrm{aa}}(\mathbf{r})$. The latter corresponds to the well-known wave function of the Cooper pairs in BCS theory. That this is a sensible way to describe the system at low temperatures, follows from the fact that it contains the correct physics in both extremes. In the extreme BEC limit the dressed molecules are just bare molecules, i.e., $Z \simeq 1$. In the BCS limit we have $Z \simeq 0$ and the dressed molecules correspond to the BCS Cooper pairs with the wave function $\chi_{\mathrm{aa}}(\mathbf{r})$. In between these two limits the probability Z changes gradually and in this manner describes the smooth crossover from the BEC to the BCS limit. This important microscopic parameter has indeed been measured recently for ^{6}Li by Partridge et al. [10] and was shortly thereafter calculated theoretically for that case in Ref. [28].

The paper is organized as follows. Because of its importance for the many-body theory that is of most interest to us, we first briefly discuss in Sec. II the atomic physics that is required to account for the resonant interactions between two atoms. In particular, we give a simple two-body derivation of the probability Z, that is then generalized in Sec. III when we discuss in detail the many-body Bogoliubov theory for the Bose-Einstein condensation of the Feshbach molecules. In Sec. IV we apply the theory to the broad Feshbach resonance of ^{6}Li at a magnetic field of $B_0 = 834$ G. We here present results for the probability Z, the spectral function of the molecules, and the speed of sound in the gas throughout the BEC-BCS crossover. In Sec. V we briefly discuss the qualitative difference that would occur in these quantities if the Feshbach resonance in ^{6}Li would be much narrower. In Sec. VI we consider the BEC, unitarity, and BCS limits of the theory. We end our paper in Sec. VII with some discussion and conclusions.

II. TWO-BODY PHYSICS AND BACKGROUND SCATTERING

For several reasons it is most convenient to start with the discussion of the relevant two-body physics of the Feshbach resonance. First, it is a natural way to introduce the probability Z, that describes the exact bound state wave function of the two-body Hamiltonian. Second, it gives a quantitative description for the problem that works quite well in the BEC-limit, where there are no free atoms in the gas and the Bose-Einstein condensate of dressed molecules is well described by two-body physics. Third, it illustrates how to incorporate not only the resonant scattering, but also the background scattering of the atoms, which turns out to be very important in the case of the extremely broad Feshbach resonance in ^{6}Li of interest to us.

For two atoms, we can simplify the Feshbach problem by first splitting off the center-of-mass motion. In that manner we arrive at the time-independent two-channel Schrödinger equation

$$\begin{pmatrix} H_{\mathrm{aa}} & V_{\mathrm{am}} \\ V_{\mathrm{am}} & \delta_B \end{pmatrix} \begin{pmatrix} |\psi_{\mathrm{a}}\rangle \\ |\psi_{\mathrm{m}}\rangle \end{pmatrix} = E \begin{pmatrix} |\psi_{\mathrm{a}}\rangle \\ |\psi_{\mathrm{m}}\rangle \end{pmatrix}, \qquad (2)$$

where $H_{\mathrm{aa}} = -\hbar^2 \boldsymbol{\nabla}^2/m + V_{\mathrm{bg}}(\mathbf{r})$ is the Hamiltonian of the relative motion in the presence of the background interaction $V_{\mathrm{bg}}(\mathbf{r})$, $|\psi_{\mathrm{a}}\rangle$ is the component of the two-body wave function in the open (triplet) channel, and $|\psi_{\mathrm{m}}\rangle$ is the component of the two-body wave function in the closed (singlet) channel. The bare detuning from resonance is given by δ_B, and V_{am} is the coupling between the open and closed channels. We formally eliminate $|\psi_{\mathrm{a}}\rangle$ from Eq. (2), by making use of the fact that the energy of the exact molecular bound state that we want to determine never lies in the spectrum of the atomic Hamiltonian H_{aa}, and insert a complete set of states in the resulting expression. In the case of a large and positive background scattering length, there exists a bound state $|\psi_{\mathrm{b}}\rangle$ just below the threshold of the scattering continuum of the atomic Hamiltonian H_{aa}. Since this bound state may be relevant we include it explicitly as well. In this manner we ultimately find

$$\begin{aligned} E - \delta_B &= \langle \psi_{\mathrm{m}} | V_{\mathrm{am}} \frac{1}{E - H_{\mathrm{aa}}} V_{\mathrm{am}} | \psi_{\mathrm{m}} \rangle \\ &= \int \frac{d^3\mathbf{k}}{(2\pi)^3} \langle \psi_{\mathrm{m}} | V_{\mathrm{am}} | \psi_{\mathbf{k}}^{(+)} \rangle \frac{1}{E - 2\epsilon_{\mathbf{k}}} \langle \psi_{\mathbf{k}}^{(+)} | V_{\mathrm{am}} | \psi_{\mathrm{m}} \rangle \\ &\quad + \langle \psi_{\mathrm{m}} | V_{\mathrm{am}} | \psi_{\mathrm{b}} \rangle \frac{1}{E - E_{\mathrm{b}}} \langle \psi_{\mathrm{b}} | V_{\mathrm{am}} | \psi_{\mathrm{m}} \rangle, \end{aligned} \qquad (3)$$

where $2\epsilon_{\mathbf{k}} = \hbar^2 \mathbf{k}^2/m$ are the energies of the atomic scattering states $|\psi_{\mathbf{k}}^{(+)}\rangle$. We focus on the first term in the right-hand side of Eq. (3) that is due to the continuum of scattering states, and leave the second term due to the bound state for later.

We would like to use the pseudopotential approximation for the matrix element $\langle \psi_{\mathrm{m}} | V_{\mathrm{am}} | \psi_{\mathbf{k}}^{(+)} \rangle$. Therefore, we rewrite the first term by using the definition of the two-body T-matrix $V_{\mathrm{bg}} | \psi_{\mathbf{k}}^{(+)} \rangle \equiv T_{\mathrm{bg}}(2\epsilon_{\mathbf{k}}) | \mathbf{k} \rangle$, where $|\mathbf{k}\rangle$ denotes the incoming plane-wave state associated with the scattering state $|\psi_{\mathbf{k}}^{(+)}\rangle$. We thus obtain

$$\begin{aligned} &\langle \psi_{\mathrm{m}} | V_{\mathrm{am}} | \psi_{\mathbf{k}}^{(+)} \rangle \\ &= \int \frac{d^3\mathbf{k}'}{(2\pi)^3} \langle \psi_{\mathrm{m}} | V_{\mathrm{am}} V_{\mathrm{bg}}^{-1} | \mathbf{k}' \rangle \langle \mathbf{k}' | T_{\mathrm{bg}}(2\epsilon_{\mathbf{k}}) | \mathbf{k} \rangle. \end{aligned} \qquad (4)$$

For long wavelengths, the scattering properties of any interatomic potential become hard-core like, as the incoming particles have too low energies to probe the structure of the interaction potential. The background scattering is then described by a single parameter, the background scattering length a_{bg}. Moreover, the conservation of probability then leads to the simply result $\langle \mathbf{k}' | T_{\mathrm{bg}}(2\epsilon_{\mathbf{k}}) | \mathbf{k} \rangle \simeq 4\pi a_{\mathrm{bg}} \hbar^2/m(1 + ika_{\mathrm{bg}})$. As a result, we

can introduce the coupling parameter g, that describes the coupling between the two channels by means of

$$\langle \psi_{\mathrm{m}} | V_{\mathrm{am}} | \psi_{\mathbf{k}}^{(+)} \rangle \equiv \frac{g}{1 + ika_{\mathrm{bg}}}. \tag{5}$$

Hence the continuum contribution in the right-hand side of Eq. (3) is

$$g^2 \int \frac{d^3\mathbf{k}}{(2\pi)^3} \frac{1}{1 + (ka_{\mathrm{bg}})^2} \frac{1}{E - 2\epsilon_{\mathbf{k}}}. \tag{6}$$

The zero-energy limit of this expression leads in Eq. (3) to a (finite) renormalization of the bare detuning δ_B to the experimentally observable detuning $\delta = \Delta\mu(B - B_0)$ that is exactly zero on resonance. Here $\Delta\mu$ denotes the magnetic-moment difference between the open and closed channels of the Feshbach resonance. For ^{6}Li we have $\Delta\mu \simeq 2\mu_B$ in terms of the Bohr magneton μ_B. Subtracting this limiting value we have that

$$\begin{aligned} \hbar\Sigma_{\mathrm{m}}(E) &= g^2 \int \frac{d^3\mathbf{k}}{(2\pi)^3} \frac{1}{1 + (ka_{\mathrm{bg}})^2} \left(\frac{1}{E - 2\epsilon_{\mathbf{k}}} + \frac{1}{2\epsilon_{\mathbf{k}}} \right) \\ &= \eta \frac{\sqrt{-E}}{1 + \frac{|a_{\mathrm{bg}}|\sqrt{m}}{\hbar}\sqrt{-E}}, \end{aligned} \tag{7}$$

with $\eta = g^2 m^{3/2}/4\pi\hbar^3$ [29]. We have written $\hbar\Sigma_{\mathrm{m}}(E)$ to indicate that this term gives the self-energy of the molecules, which follows from the fact that the energy of the exact molecular bound state is found from

$$E = \delta + \hbar\Sigma_{\mathrm{m}}(E). \tag{8}$$

Now we wish to include also the bound state in the case of a large and positive background scattering length. For the moment we do not assume that the bound-state energy lies at $-\hbar^2/ma_{\mathrm{bg}}^2$, but we initially use $E_{\mathrm{b}} = -\hbar^2/ma_{\mathrm{b}}^2$, where a_{b} may be different from a_{bg} due to effective-range effects. To determine the contribution of the bound state, we compare the normalizations of the wave functions of the bound and scattering states. We have in the pseudopotential approximation that

$$\psi_{\mathbf{0}}^{(+)}(\mathbf{r}) = \left(1 - \frac{a_{\mathrm{bg}}}{r}\right), \tag{9}$$

$$\psi_{\mathrm{b}}(\mathbf{r}) = \frac{1}{\sqrt{2\pi a_{\mathrm{b}}}} \frac{e^{-r/a_{\mathrm{b}}}}{r}, \tag{10}$$

which implies that for small separations between the atoms

$$\psi_{\mathrm{b}}(\mathbf{r}) = -\frac{1}{\sqrt{2\pi a_{\mathrm{bg}}^2 a_{\mathrm{b}}}} \psi_{\mathbf{0}}^{(+)}(\mathbf{r}). \tag{11}$$

We can now use the results of Eqs. (11) and (5) to calculate the self-energy contribution of the bound state. Subtracting again the zero-energy limit to renormalize the bare detuning δ_B we find now

$$\hbar\Sigma_{\mathrm{m}}(E) = \eta \left[\frac{\sqrt{-E}}{1 + \frac{|a_{\mathrm{bg}}|\sqrt{m}}{\hbar}\sqrt{-E}} - \frac{2\hbar^2/ma_{\mathrm{bg}}^2}{\sqrt{-E_{\mathrm{b}}}} \frac{1}{1 - E_{\mathrm{b}}/E} \right]. \tag{12}$$

Using this result we can show that if $E_{\mathrm{b}} = -\hbar^2/ma_{\mathrm{bg}}^2$ we have

$$\hbar\Sigma_{\mathrm{m}}(E) = \eta \frac{\sqrt{-E}}{1 - \frac{a_{\mathrm{bg}}\sqrt{m}}{\hbar}\sqrt{-E}}. \tag{13}$$

Note that compared to Eq. (7) the bound-state contribution has in the limit of a very large positive background scattering length resulted in the simple replacement $|a_{\mathrm{bg}}| \to -a_{\mathrm{bg}}$, which shows that the precise value of the energy of the bound state is all important in determining whether the combined effect of the scattering continuum and the bound state shifts the dressed molecular energy up or down. Using Eqs. (8) and (12) we can find the binding energy of the dressed molecule in the 2-body limit. We have applied this result to measurements of the binding energy of ^{40}K molecules [30] and find excellent agreement with experiment as shown in Fig. 1. It is interesting that in this case the binding energy $-E_{\mathrm{b}}$ is substantially larger than $\hbar^2/ma_{\mathrm{bg}}^2$ and it is therefore a better approximation to use Eq. (7) for the molecular self-energy than Eq. (13). The use of the latter self-energy would shift the molecular binding energies upward compared to the result with no background interactions, whereas agreement with the experimental results requires a downward shift.
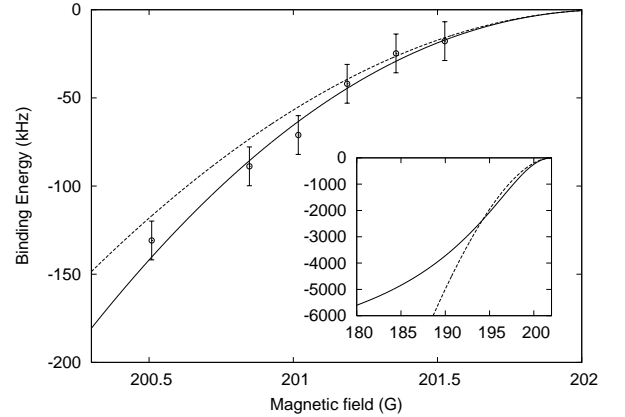

FIG. 1: Binding energies for the dressed molecules as a function of magnetic field. The solid line is given by the solution of Eqs. (8) and (12), where we have used $E_{\mathrm{b}} = -8.9$ MHz for the bound-state energy in the background potential [31]. The dashed line is the solution in the absence of background interactions. The points are from the experiment of Moritz *et al.* [30]. The inset shows how the binding energy behaves as the energy of the bound state in the background potential is approached and an avoided crossing occurs.

Now we can go back to the quantity Z that describes the closed-channel component of the dressed molecule as in Eq. (1). While calculating the self-energy of the molecules, we have used a normalization such that $\langle \psi_{\mathrm{m}} | \psi_{\mathrm{m}} \rangle = 1$. This implies that the normalization of the atomic part of the dressed molecular wave function

equals $(1-Z)/Z$, so we have the relation

$$
\begin{aligned}
\frac{1-Z}{Z} &= \langle\psi_{\mathrm{a}}|\psi_{\mathrm{a}}\rangle \\
&= \langle\psi_{\mathrm{m}}|V_{\mathrm{am}}\frac{1}{(E-H_{\mathrm{a}})^2}V_{\mathrm{am}}|\psi_{\mathrm{m}}\rangle\Big|_{E=\epsilon_{\mathrm{m}}(\delta)} \\
&= -\frac{\partial\hbar\Sigma_{\mathrm{m}}(E)}{\partial E}\Big|_{E=\epsilon_{\mathrm{m}}(\delta)}, \quad\quad (14)
\end{aligned}
$$

where $\epsilon_{\mathrm{m}}(\delta)$ is the energy of the exact dressed molecular state and the solution of the equation $\epsilon_{\mathrm{m}} = \delta + \hbar\Sigma_{\mathrm{m}}(\epsilon_{\mathrm{m}})$. From this relation it follows that

$$
Z = \left[1-\frac{\partial\hbar\Sigma_{\mathrm{m}}(E)}{\partial E}\right]^{-1}\Bigg|_{E=\epsilon_{\mathrm{m}}(\delta)}. \quad\quad (15)
$$

The probability Z of the dressed molecule to be in the closed-channel state was measured in the experiments of Jochim *et al.* [32] and Partridge *et al.* [10] for ^{6}Li. Using the two-body results derived so far, we can get a very good agreement on the BEC-side of the resonance, as is shown in Fig. 2. At the two-body level, no stable molecules exist for positive detuning. Moreover, in that case Z becomes zero exactly at the resonance. Both features disappear at the many-body level as we discuss in detail in the next section.
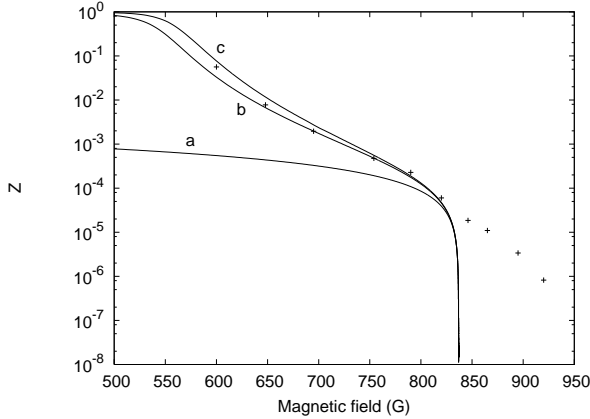

FIG. 2: The two-body Z as a function of magnetic field for ^{6}Li, (a) without background interactions, (b) with a constant background scattering length $a_{\mathrm{bg}} = -1360a_0$ equal to the background scattering length at resonance, and (c) with a magnetic field-dependent background scattering length as determined in Ref. [33]. The points are from the experiment of Partridge *et al.* [10].

III. BOGOLIUBOV THEORY OF MOLECULES

In this section we give a detailed derivation of the Bogoliubov or RPA theory of the BEC-BCS crossover. We discuss the problems that arise when trying to numerically calculate the fluctuation corrections. We also consider the long-wavelength limit of the theory.

A. Equation of state

We start the development of the Bogoliubov theory by introducing the annihilation operator $\psi_{\mathrm{m}}(\mathbf{x})$ for the bare molecules, and the annihilation operators $\psi_{\uparrow}(\mathbf{x})$ and $\psi_{\downarrow}(\mathbf{x})$ for the atoms in the two different hyperfine states $|\uparrow\rangle$ and $|\downarrow\rangle$, respectively. The Hamiltonian can then be expressed in second quantization as [29, 34, 35]

$$
H = \int d\mathbf{x}\,\psi_{\mathrm{m}}^\dagger(\mathbf{x})\left(-\frac{\hbar^2\boldsymbol{\nabla}^2}{4m}+\delta_B-2\mu\right)\psi_{\mathrm{m}}(\mathbf{x}) \quad (16)
$$

$$
+\sum_{\sigma=\uparrow,\downarrow}\int d\mathbf{x}\,\psi_\sigma^\dagger(\mathbf{x})\left(-\frac{\hbar^2\boldsymbol{\nabla}^2}{2m}-\mu\right)\psi_\sigma(\mathbf{x})
$$

$$
+g\int d\mathbf{x}\left(\psi_{\mathrm{m}}^\dagger(\mathbf{x})\psi_\uparrow(\mathbf{x})\psi_\downarrow(\mathbf{x})+\psi_\downarrow^\dagger(\mathbf{x})\psi_\uparrow^\dagger(\mathbf{x})\psi_{\mathrm{m}}(\mathbf{x})\right)
$$

$$
+\frac{4\pi a_{\mathrm{bg}}\hbar^2}{m}\int d\mathbf{x}\,\psi_\downarrow^\dagger(\mathbf{x})\psi_\uparrow^\dagger(\mathbf{x})\psi_\uparrow(\mathbf{x})\psi_\downarrow(\mathbf{x}). \quad (17)
$$

We use functional methods to calculate the physical quantities of interest, as it is simpler than the operator formalism when going beyond mean-field theory. In the end, both the two-body physics, that we treated in the previous section, as well as the many-body BEC-BCS crossover physics are incorporated in our theory. This is achieved by first writing down the grand-canonical partition function of the gas as the functional integral

$$
Z_{\mathrm{gr}} = \int d[\psi_{\mathrm{m}}^*]d[\psi_{\mathrm{m}}]d[\psi_\sigma^*]d[\psi_\sigma]e^{-S[\psi_{\mathrm{m}}^*,\psi_{\mathrm{m}},\psi_\sigma^*,\psi_\sigma]/\hbar}, \quad (18)
$$

where the Euclidean or imaginary-time action is

$$
\begin{aligned}
S[\psi_{\mathrm{m}}^*,\psi_{\mathrm{m}},\psi_\sigma^*,\psi_\sigma] = \int_0^{\hbar\beta}d\tau\Bigg\{&H[\psi_{\mathrm{m}}^*,\psi_{\mathrm{m}},\psi_\sigma^*,\psi_\sigma] \\
&+\sum_{\sigma=\uparrow,\downarrow}\int d\mathbf{x}\,\psi_\sigma^*(\mathbf{x},\tau)\hbar\frac{\partial}{\partial\tau}\psi_\sigma(\mathbf{x},\tau) \\
&+\int d\mathbf{x}\,\psi_{\mathrm{m}}^*(\mathbf{x},\tau)\hbar\frac{\partial}{\partial\tau}\psi_{\mathrm{m}}(\mathbf{x},\tau)\Bigg\}. \quad (19)
\end{aligned}
$$

We then rewrite the open-channel part of this action using Green's function methods, where the Green's function $G(\mathbf{x},\tau;\mathbf{x}',\tau')$ can be seen as a 'matrix' with space and time 'indices'. We obtain

$$
\begin{aligned}
S = &\int d\tau\,d\mathbf{x}\,\psi_{\mathrm{m}}^*(\mathbf{x},\tau)\left(\hbar\frac{\partial}{\partial\tau}-\frac{\hbar^2\nabla^2}{4m}+\delta_B-2\mu\right)\psi_{\mathrm{m}}(\mathbf{x},\tau) \\
&-\int d\tau\,d\mathbf{x}\,d\tau'\,d\mathbf{x}'\,[\psi_\downarrow^*(\mathbf{x},\tau),\psi_\uparrow(\mathbf{x},\tau)]\,\hbar G^{-1}\begin{bmatrix}\psi_\downarrow(\mathbf{x}',\tau')\\\psi_\uparrow^*(\mathbf{x}',\tau')\end{bmatrix}.
\end{aligned}
$$
$$(20)$$

The coupling between the atoms and the molecules is contained in the atomic 2×2 Nambu-space matrix propagator $G(\mathbf{x},\tau;\mathbf{x}',\tau')$, i.e., $G = G[\psi_{\mathrm{m}}^*,\psi_{\mathrm{m}}]$ depends on the molecular field $\psi_{\mathrm{m}}(\mathbf{x},\tau)$. This is a convenient rewrite, as it will allow us to integrate out the atoms using Gaussian integration. It also makes a clear connection with

the operator formalism, as the propagator is related to the expectation value of the imaginary-time Heisenberg operators in the following manner

$$G(\mathbf{x}, \tau; \mathbf{x}', \tau')$$
$$= -\left\langle T\left(\begin{bmatrix} \psi_\downarrow(\mathbf{x}, \tau) \\ \psi_\uparrow^\dagger(\mathbf{x}, \tau) \end{bmatrix} \begin{bmatrix} \psi_\downarrow^\dagger(\mathbf{x}', \tau'), \psi_\uparrow(\mathbf{x}', \tau') \end{bmatrix} \right)\right\rangle, \quad (21)$$

where T is the time-ordering operator. The 2x2 matrix-structure allows us for including the coupling to the molecules and in particular immediately incorporates the anomalous expectation values of the atomic gas that arise when the molecules Bose-Einstein condense.

It appears that we have neglected here the background interaction between the atoms. However, we reintroduce the effects of the background scattering on the coupling g once we go back to momentum space, which, in agreement with Eq. (5), results in the substitution $g \to g/(1 + ika_{\mathrm{bg}})$ where k is the magnitude of the relative momentum between the two atoms. Diagrammatically this procedure is shown in Fig. 3.
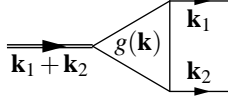
FIG. 3: Momentum-dependent atom-molecule coupling. The incoming molecular field is represented by the double lines and the single lines represent the outgoing atoms. The coupling g depends on the relative momentum $\mathbf{k} = (\mathbf{k}_2 - \mathbf{k}_1)/2$ of the outgoing atoms in the case of a non-negligible background interaction.

Our aim is to exactly integrate out the atoms and expand the result up to second order in the fluctuations of the molecular field around its expectation value $\langle \psi_{\mathrm{m}}(\mathbf{x}, \tau) \rangle$, which we assume to be real from now on, and thus arrive at a Bogoliubov theory for the bare molecules. To make the connection with BCS-theory explicit, we write $\langle \psi_{\mathrm{m}}(\mathbf{x}, \tau) \rangle = \Delta/g$, perform the substitution $\psi_{\mathrm{m}}(\mathbf{x}, \tau) \to \Delta/g + \psi_{\mathrm{m}}(\mathbf{x}, \tau)$, and use the Dyson equation

$$G^{-1} = G_{\mathrm{a}}^{-1} - \Sigma \quad (22)$$

with

$$G_{\mathrm{a}}^{-1} = -\frac{1}{\hbar} \begin{pmatrix} \hbar\frac{\partial}{\partial\tau} - \frac{\hbar^2\nabla^2}{2m} - \mu & \Delta \\ \Delta & \hbar\frac{\partial}{\partial\tau} + \frac{\hbar^2\nabla^2}{2m} + \mu \end{pmatrix}$$
$$\times \delta(\mathbf{x} - \mathbf{x}')\delta(\tau - \tau'),$$
$$\Sigma = \frac{1}{\hbar} \begin{pmatrix} 0 & g\psi_{\mathrm{m}}(\mathbf{x}, \tau) \\ g\psi_{\mathrm{m}}^*(\mathbf{x}, \tau) & 0 \end{pmatrix} \delta(\mathbf{x} - \mathbf{x}')\delta(\tau - \tau').$$
$$(23)$$

The reason for this procedure is that G_{a}^{-1} is now exactly the usual BCS propagator, which we know how to deal with exactly from BCS theory. The 'gap' Δ is in our case proportional to the expectation value of the molecular field, i.e., it represents the molecular BEC. Two atoms can be annihilated through the formation of a bare molecule in the condensate. Vice-versa, two atoms can also be created from the molecular condensate. Diagrammatically, the propagator can be expanded as is shown in Fig. 4.
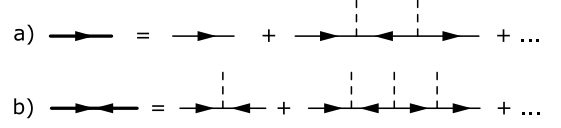
FIG. 4: Diagrammatic expansion of the normal and anomalous BCS propagators. The thick lines represent the full BCS propagator, the thin lines represent the bare propagator. Interactions with the molecular Bose-Einstein condensate are denoted by the dashed lines. a) The normal BCS propagator. b) The anomalous propagator.

The self-energy term Σ accounts for the molecular fluctuations, and as such depends on the molecular field, $\Sigma = \Sigma[\psi_{\mathrm{m}}^*, \psi_{\mathrm{m}}]$. The action has become quadratic in the atomic fields, and so we can now formally integrate out the atoms by doing the Gaussian integral. We make use of the fact that G can be seen as a matrix with space-time 'indices' and obtain

$$Z_{\mathrm{gr}} = \int d[\psi_{\mathrm{m}}^*]d[\psi_{\mathrm{m}}] \exp\left\{ -S_{\mathrm{m}}[\psi_{\mathrm{m}}^*, \psi_{\mathrm{m}}]/\hbar + \mathrm{Tr}\left[\ln(-G^{-1}[\psi_{\mathrm{m}}^*, \psi_{\mathrm{m}}])\right] \right\}, \quad (24)$$

where the trace is over Nambu space, and over the space and (imaginary) time coordinates. We next expand this exact result up to second-order in the molecular fluctuations by means of

$$\mathrm{Tr}[\ln(-G^{-1})] = \mathrm{Tr}[\ln(-G_{\mathrm{a}}^{-1}(1 - G_{\mathrm{a}}\Sigma))]$$
$$= \mathrm{Tr}[\ln(-G_{\mathrm{a}}^{-1})] - \mathrm{Tr}[G_{\mathrm{a}}\Sigma + \frac{1}{2}G_{\mathrm{a}}\Sigma G_{\mathrm{a}}\Sigma + \ldots].$$
$$(25)$$

Since the self-energy $\hbar\Sigma$ is linear in ψ_{m} this is indeed effectively an expansion in the molecular fluctuations. The first-order term, $\mathrm{Tr}[G_{\mathrm{a}}\Sigma]$, is required to be equal to $(2\mu - \delta_B)(\psi_{\mathrm{m}} + \psi_{\mathrm{m}}^*)/\hbar$ because we want to expand around the minimum of the effective action. Using the expressions for Σ and G_{a}, and going over to momentum space, the second-order term can be written in the zero-temperature limit as

$$\mathrm{Tr}\,[G_\mathrm{a}\Sigma G_\mathrm{a}\Sigma] = \sum_{\mathbf{k},n} [\psi_\mathrm{m}^*(\mathbf{k},i\omega_n),\psi_\mathrm{m}(-\mathbf{k},-i\omega_n)] \begin{bmatrix} \Sigma_{11}(\mathbf{k},i\omega_n) & \Sigma_{12}(\mathbf{k},i\omega_n) \\ \Sigma_{21}(\mathbf{k},i\omega_n) & \Sigma_{22}(\mathbf{k},i\omega_n) \end{bmatrix} \begin{bmatrix} \psi_\mathrm{m}(\mathbf{k},i\omega_n) \\ \psi_\mathrm{m}^*(-\mathbf{k},-i\omega_n) \end{bmatrix}. \tag{26}$$

For example, Σ_{11} contains two normal fermionic propagators, which can be taken from Eq. (23). In momentum space, this ultimately leads to

$$\hbar\Sigma_{11}(\mathbf{k},i\omega_n) = -\frac{1}{\beta}\int \frac{d\mathbf{k}'}{(2\pi)^3} \sum_{n'} |g(\mathbf{k}')|^2 \frac{i\hbar\omega_{n'_+} + \epsilon(\mathbf{k}'_+) - \mu}{[\hbar\omega_{n'_+}]^2 + [\hbar\omega_a(\mathbf{k}'_+)]^2}\frac{i\hbar\omega_{n'_-} + \epsilon(\mathbf{k}'_-) - \mu}{[\hbar\omega_{n'_-}]^2 + [\hbar\omega_a(\mathbf{k}'_-)]^2} \tag{27}$$

Here we have also introduced the BCS dispersion $\hbar\omega_\mathrm{a}(\mathbf{k}) = [(\epsilon(\mathbf{k}) - \mu)^2 + \Delta^2/(1 + a_\mathrm{bg}^2\mathbf{k}^2)]^{1/2}$, the atomic dispersion $\epsilon(\mathbf{k}) = \hbar^2\mathbf{k}^2/2m$, and the notation $\mathbf{k}'_\pm = \mathbf{k}/2 \pm \mathbf{k}'$ and $n'_\pm = n/2 \pm n'$. The coupling g is dressed by the background scattering through $|g(\mathbf{k})|^2 = g^2/(1 + \mathbf{k}^2 a_\mathrm{bg}^2)$ as explained previously. The two propagators can be reduced using partial fraction decomposition, resulting in the expression

$$\begin{aligned}
\hbar\Sigma_{11}(\mathbf{k},i\omega_n) = \frac{1}{\beta}\int \frac{d\mathbf{k}'}{(2\pi)^3} \sum_{n'} |g(\mathbf{k}')|^2 \Bigg\{ & \frac{u_\mathrm{a}^2(\mathbf{k}'_+)u_\mathrm{a}^2(\mathbf{k}'_-)}{\hbar\omega_\mathrm{a}(\mathbf{k}'_+) + \hbar\omega_\mathrm{a}(\mathbf{k}'_-) - i\hbar\omega_n}\left[\frac{1}{i\hbar\omega_{n'_+} - \hbar\omega_\mathrm{a}(\mathbf{k}'_+)} + \frac{1}{i\hbar\omega_{n'_-} - \hbar\omega_\mathrm{a}(\mathbf{k}'_-)}\right] \\
& + \frac{u_\mathrm{a}^2(\mathbf{k}'_+)v_\mathrm{a}^2(\mathbf{k}'_-)}{\hbar\omega_\mathrm{a}(\mathbf{k}'_+) - \hbar\omega_\mathrm{a}(\mathbf{k}'_-) - i\hbar\omega_n}\left[\frac{1}{i\hbar\omega_{n'_+} - \hbar\omega_\mathrm{a}(\mathbf{k}'_+)} + \frac{1}{i\hbar\omega_{n'_-} + \hbar\omega_\mathrm{a}(\mathbf{k}'_-)}\right] \\
& + \frac{v_\mathrm{a}^2(\mathbf{k}'_+)u_\mathrm{a}^2(\mathbf{k}'_-)}{-\hbar\omega_\mathrm{a}(\mathbf{k}'_+) + \hbar\omega_\mathrm{a}(\mathbf{k}'_-) - i\hbar\omega_n}\left[\frac{1}{i\hbar\omega_{n'_+} + \hbar\omega_\mathrm{a}(\mathbf{k}'_+)} + \frac{1}{i\hbar\omega_{n'_-} - \hbar\omega_\mathrm{a}(\mathbf{k}'_-)}\right] \\
& + \frac{v_\mathrm{a}^2(\mathbf{k}'_+)v_\mathrm{a}^2(\mathbf{k}'_-)}{-\hbar\omega_\mathrm{a}(\mathbf{k}'_+) - \hbar\omega_\mathrm{a}(\mathbf{k}'_-) - i\hbar\omega_n}\left[\frac{1}{i\hbar\omega_{n'_+} + \hbar\omega_\mathrm{a}(\mathbf{k}'_+)} + \frac{1}{i\hbar\omega_{n'_-} + \hbar\omega_\mathrm{a}(\mathbf{k}'_-)}\right] \Bigg\},
\end{aligned} \tag{28}$$

where $u_\mathrm{a}(\mathbf{k})$ and $v_\mathrm{a}(\mathbf{k})$ are the usual BCS coherence factors, obeying

$$u_\mathrm{a}^2(\mathbf{k}) = \frac{\hbar\omega_\mathrm{a}(\mathbf{k}) + \epsilon(\mathbf{k}) - \mu}{2\hbar\omega_\mathrm{a}(\mathbf{k})}, \tag{29}$$

$$v_\mathrm{a}^2(\mathbf{k}) = \frac{\hbar\omega_\mathrm{a}(\mathbf{k}) - \epsilon(\mathbf{k}) + \mu}{2\hbar\omega_\mathrm{a}(\mathbf{k})}. \tag{30}$$

From the terms in the right-hand side of Eq. (28), we can read off the different processes that lead to a dressing of the bare molecules. The ladder diagram which this expression corresponds to is shown in Fig. 5a. It describes two fermions, propagating with momentum $\mathbf{k}_+$ and $\mathbf{k}_-$. In the BCS-picture, there are indeed four possible pro-cesses that renormalize the molecules, due to the possibility for the molecules to break up into two quasi-particles (proportional to $u_\mathrm{a}^2 u_\mathrm{a}^2$), a quasi-hole and a quasi-particle (proportional to $u_\mathrm{a}^2 v_\mathrm{a}^2$), or two quasi-holes (proportional to $v_\mathrm{a}^2 v_\mathrm{a}^2$).

Next, we take the zero-temperature limit by replacing the sum over internal Matsubara frequencies n' by an integral. As a result, only two processes survive: the creation of a quasi-particle pair, and the creation of a quasi-hole pair. Finally, we perform the same renormalization of the detuning as explained in Sec. II. In this manner we are ensured that $\delta = 0$ corresponds also in the many-body theory exactly to the location of the Feshbach resonance. To conclude, the self-energy contributions are now

$$\begin{aligned}
\hbar\Sigma_{11}(\mathbf{k},i\omega_n) &= \int \frac{d\mathbf{k}'}{(2\pi)^3}\,|g(\mathbf{k}')|^2 \Bigg\{\frac{u_\mathrm{a}^2(\mathbf{k}'_+)u_\mathrm{a}^2(\mathbf{k}'_-)}{i\hbar\omega_n - \hbar\omega_\mathrm{a}(\mathbf{k}'_+) - \hbar\omega_\mathrm{a}(\mathbf{k}'_-)} - \frac{v_\mathrm{a}^2(\mathbf{k}'_+)v_\mathrm{a}^2(\mathbf{k}'_-)}{i\hbar\omega_n + \hbar\omega_\mathrm{a}(\mathbf{k}'_+) + \hbar\omega_\mathrm{a}(\mathbf{k}'_-)} + \frac{1}{2\epsilon(\mathbf{k}')}\Bigg\}, \\
\hbar\Sigma_{12}(\mathbf{k},i\omega_n) &= 2\int \frac{d\mathbf{k}'}{(2\pi)^3}\,|g(\mathbf{k}')|^2 \Bigg\{u_\mathrm{a}(\mathbf{k}'_+)v_\mathrm{a}(\mathbf{k}'_+)u_\mathrm{a}(\mathbf{k}'_-)v_\mathrm{a}(\mathbf{k}'_-)\frac{\hbar\omega_\mathrm{a}(\mathbf{k}'_+) + \hbar\omega_\mathrm{a}(\mathbf{k}'_-)}{(\hbar\omega_\mathrm{a}(\mathbf{k}'_+) + \hbar\omega_\mathrm{a}(\mathbf{k}'_-))^2 + (\hbar\omega_n)^2}\Bigg\}, \\
\hbar\Sigma_{22}(\mathbf{k},i\omega_n) &= \hbar\Sigma_{11}(\mathbf{k},-i\omega_n), \\
\hbar\Sigma_{21}(\mathbf{k},i\omega_n) &= \hbar\Sigma_{12}(\mathbf{k},-i\omega_n).
\end{aligned} \tag{31}$$

In our calculations, we also take into account that the background scattering length $a_\mathrm{bg}(B)$ and the coupling

$g(B)$ depend on the magnetic field, which turns out to be very important for the extremely broad Feshbach resonance used in all experiments with ^{6}Li [33].

Diagrammatically, Fig. 5 illustrates the way the BCS propagators are included into the theory. The ladder diagram in a) is the normal self-energy $\hbar\Sigma_{11}$. The BCS-propagators can be expanded as is shown in Fig. 4, which gives rise to contributions such as the one in c). The diagram in b) is the anomalous self-energy $\hbar\Sigma_{12}$. A contribution using bare propagators is shown in d). This shows explicitly that there is only an anomalous contribution for nonzero Δ.
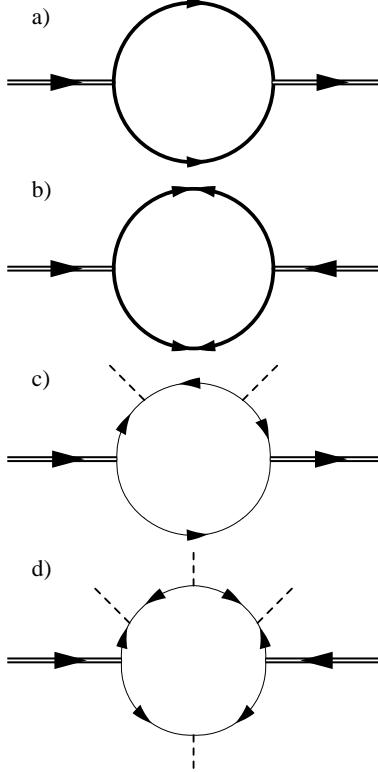
FIG. 5: Diagrammatic representation of the molecular self-energy diagrams. The bare fermionic propagators are dressed through interactions with the molecular condensate. Single lines denote fermions, double lines denote molecules. For the fermions, the thin lines represent the bare propagator, thick lines represent the BCS propagator, as in Fig. 4. Interactions with the condensate are denoted by the vertices containing a dashed line. The effect of the background scattering on the vertices is not drawn explicitly. a) The normal self-energy $\hbar\Sigma_{11}$. b) The anomalous self-energy $\hbar\Sigma_{12}$. c) An example of a contribution to the normal self-energy $\hbar\Sigma_{11}$. d) An example of a contribution to the anomalous self-energy $\hbar\Sigma_{12}$.

In terms of the above self-energies, the bare molecular condensate density Δ/g is determined by the exact Hugenholtz-Pines relation $2\mu = \delta + \hbar\Sigma_{11}(\mathbf{0},0) - \hbar\Sigma_{12}(\mathbf{0},0)$ [36], which in our case turns out to be equal

to the modified BCS gap equation

$$\delta - 2\mu = \int \frac{d\mathbf{k}}{(2\pi)^3}\, |g(\mathbf{k})|^2 \left(\frac{1}{2\hbar\omega_{\mathrm{a}}(\mathbf{k})} - \frac{1}{2\epsilon(\mathbf{k})} \right). \quad (32)$$

As expected, the same gap equation can also be obtained from the requirement that the linear terms $(\delta_B - 2\mu)(\psi_{\mathrm{m}} + \psi_{\mathrm{m}}^*) + \mathrm{Tr}[G_{\mathrm{a}}\hbar\Sigma]$ in the effective molecular action vanish.

Integrating out the atoms has led to an effective Bogoliubov action for the bare molecules. The interaction effects between the molecules and atoms are contained in the normal and anomalous self-energies $\hbar\Sigma_{ij}$. Because we have expanded in the molecular fluctuations only, the BCS propagators for the atomic fields are included everywhere, and the BCS state is fully incorporated in the physics. Beyond that, we have constructed an effective action that also describes the fluctuations or noncondensed molecules, which serves to draw not only conclusions about the condensate depletion but also on the nature of the dressed molecules in the condensate as we will see in a moment.

The inverse propagator of the molecules takes the form

$$-\hbar G_{\mathrm{m}}^{-1} = \begin{bmatrix} -\hbar G_{11}^{-1} + \hbar\Sigma_{11} & \hbar\Sigma_{12} \\ \hbar\Sigma_{21} & -\hbar G_{22}^{-1} + \hbar\Sigma_{22} \end{bmatrix}, \quad (33)$$

where

$$\begin{aligned} -\hbar G_{11}^{-1}(\mathbf{k}, i\omega) &= -i\hbar\omega + \epsilon(\mathbf{k})/2 + \delta - 2\mu, \\ -\hbar G_{22}^{-1}(\mathbf{k}, i\omega) &= i\hbar\omega + \epsilon(\mathbf{k})/2 + \delta - 2\mu \end{aligned} \quad (34)$$

are taken from Eq. (20). The molecular propagator can be written as the expectation value of time-ordered molecular creation and annihilation operators, similarly as the atomic propagator in Eq. (21). Using these expressions we can obtain the grand-canonical partition function Z_{gr} and the thermodynamic potential $\Omega = -\ln(Z_{\mathrm{gr}})/\beta$ in the Bogoliubov approximation by performing the Gaussian integral over the molecular fluctuations. Ultimately we obtain in this manner

$$\begin{aligned} Z_{\mathrm{gr}} = \exp &\left\{ \mathrm{Tr}\left[\ln(-G_{\mathrm{a}}^{-1}) \right] - \frac{1}{2}\mathrm{Tr}\left[\ln(-G_{\mathrm{m}}^{-1}) \right] \right. \\ &\left. - \beta(\delta - 2\mu)V\frac{|\Delta|^2}{g^2} \right\}, \end{aligned} \quad (35)$$

where V is the volume of the gas. As the molecular and atomic contributions have now mixed, it is appropriate to determine the equation of state by taking the derivative of the thermodynamic potential with respect to the chemical potential. Hence, the total atomic density be-

comes

$$n = -\frac{1}{V}\frac{\partial \Omega}{\partial \mu}$$

$$= \frac{1}{\hbar \beta V}\text{Tr}\left[G_a \sigma_3\right] + \frac{2\Delta^2}{g^2} - \frac{1}{2\beta V}\text{Tr}\left[\frac{G_m}{\hbar}\frac{\partial \hbar G_m^{-1}}{\partial \mu}\right]$$

$$= \frac{2}{V}\sum_{\mathbf{k}}|v_a(\mathbf{k})|^2 + \frac{2\Delta^2}{g^2} - \frac{1}{\hbar \beta V}\text{Tr}\left[G_m\right]$$

$$+ \frac{1}{2\hbar \beta V}\text{Tr}\left[G_m \frac{\partial \hbar \Sigma}{\partial \mu}\right]. \tag{36}$$

Here the third Pauli matrix in Nambu space is denoted by σ_3. Because we are working at zero temperature and in the thermodynamic limit, we can rewrite the trace as an integral over momenta and frequencies. In detail this means that $\sum_{\mathbf{k},n}/\hbar \beta V = \int d\omega d\mathbf{k}/(2\pi)^4$.

The four terms in the right-hand side of Eq. (36) have the following physical interpretation. The first term is the usual BCS expression for the density of atoms in the BCS ground state. The second term gives the contribution of the bare molecular Bose-Einstein condensate to the total atomic density, and the third term gives the contribution of the bare molecules that are not Bose-Einstein condensed, i.e., it describes the depletion of the bare molecular Bose-Einstein condensate. The fourth and last term is most difficult to understand and can be best explained by reformulating the equation of state in terms of dressed molecules instead of bare molecules. If the gas contains a Bose-Einstein condensate of dressed molecules, there is both a bare molecular contribution and an atomic contribution to the total atomic density of the Bose-Einstein condensate. These two contributions, together with the contribution of the unpaired atoms, are contained in the first two terms in the right-hand side of Eq. (36). These two terms correspond to the mean-field theory of the BEC-BCS crossover. The third and the fourth terms in the right-hand side of Eq. (36) represent the effects of fluctuations. Together they give essentially the bare molecular contribution and the atomic contribution to the total atomic density of the dressed molecules that are not Bose-Einstein condensed. In the Bogoliubov theory, therefore, the gas consists of unpaired atoms, Bose-Einstein condensed dressed molecules, and dressed molecules that are not Bose-Einstein condensed.

B. Numerical methods

Though the analytical expressions for our theory are quite compact and their behavior can be studied in all limits, solving the gap equation in Eq. (32) and the equation of state in Eq. (36) simultaneously is quite involved. It is important to examine these equations carefully, in order to avoid numerical difficulties. It should be noted that the integrand of the self-energy not only depends on the magnitudes of the internal and external momenta, but also on the angle between them, so the integration

over internal momenta is in fact a two-dimensional one. In combination with the integration over the external momenta and Matsubara frequencies and the iteration procedure required to find a self-consistent solution at all magnetic fields, this leads to the practical necessity of choosing a fast method of calculation where possible. Convergence issues turn also out to be a problem, especially in the case of a broad resonance.

Our general procedure is to solve the gap equation and the equation of state iteratively, to find the desired value of the total atomic density. The input for this procedure is the gap Δ, which is completely fixed during the iterations. Then we take a chemical potential, and solve the gap equation to find the detuning. Finally, the equation of state gives the atomic density that we can compare with the desired experimental density. We adjust the chemical potential appropriately, and start the next iteration. We perform this procedure for different Δ to obtain a self-consistent solution for various values of the magnetic field. The reason why we keep Δ fixed rather than the detuning, is that this ensures that a physical solution of the gap equation can always be found.

We have found that the procedure of tracing over the Matsubara frequencies is very subtle. The first possibility of doing this is to just replace the discrete sum by an integral, due to the zero-temperature limit, and to perform a straightforward integration over the frequencies along the imaginary axis of the complex frequency plane. This is shown in Fig. 6 by the solid curve. In this figure, the frequencies are shown as a complex energy $z = i\hbar\omega_n$. Using this method, we calculate the equal-time propagators $\sum_n G(\mathbf{k}, i\omega_n) = N(\mathbf{k}) + 1/2$, and therefore a convergence factor is needed to obtain the correct occupation number $N(\mathbf{k})$. This is equivalent to closing the contour on the left with a large semicircle.
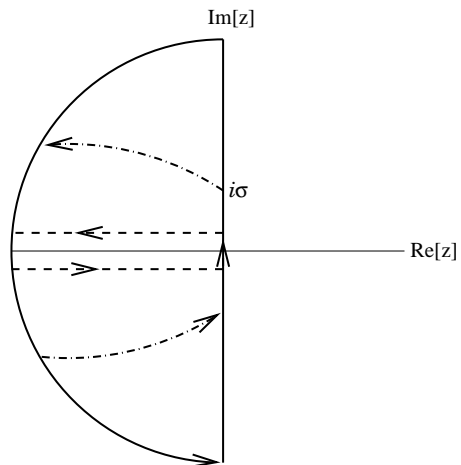

FIG. 6: Tracing the Matsubara frequencies using various methods of contour integration.

For the third and fourth terms in the right-hand side of Eq. (36) this method has a significant disadvantage.

In particular, for the third term and for high external momenta, the integration over the imaginary axis, and the closing of the contour add to zero, and this means the calculation would be very sensitive to the precision with which these contributions can be calculated.

An alternative is to perform a contour deformation, such that the path of integration lies infinitesimally below and above the real axis, as is shown by the dashed lines in Fig. 6. This is usually a desirable method, as there is no need to correct for the value of the equal-time propagators. The use of this method, however, necessitates knowledge of the analytic structure of the retarded propagator to accurately perform the numerical integration, which is not feasible to obtain from our complicated expressions for the self-energy. Therefore, we prefer to use another method by integrating over some intermediate path, and to work with complex energies along the integration. Any parabolic shape would seem very suitable, as it also takes away the need for closing the contour on the left side. Unfortunately, these curves have a strong positive and negative contribution over a wide range of energies, that would again have to cancel.

For the third term in the right-hand side of Eq. (36), the best approach, shown by the dash-dotted line in Fig. 6, is to go along the imaginary axis for a finite interval σ, and then to follow a special path given by

$$
\begin{aligned}
z(p) = & \epsilon(\mathbf{k})/2 - 2\mu \\
& - \left[(p+1)\sqrt{\epsilon(\mathbf{k})/2 - 2\mu - i\sigma} + p\eta \right]^2,
\end{aligned} \tag{37}
$$

where p parametrizes the path and $\epsilon(\mathbf{k})$ is the external momentum. This expression is chosen such that the two-body self-energy would give exactly zero along the path. Closing the contour still gives a correction of

$$
\frac{4}{\pi} \mathrm{Arg}\left[\eta + \sqrt{\epsilon(\mathbf{k})/2 - 2\mu - i\sigma} \right], \tag{38}
$$

where $\mathrm{Arg}[z]$ gives the argument of the complex number z. This term becomes small for small σ and large $\epsilon(\mathbf{k})$. For the fourth term in the right-hand side of Eq. (36), such a procedure is not possible, and we resort to a parabolic path around the negative real axis. In this case, the convergence is better, as the integrand behaves as $1/|z|^2$.

C. Long-wavelength limit

We finally study the behavior of the poles of the bare molecular propagator. The molecular propagator at zero momentum describes the closed-channel part of the Bose-Einstein condensate of dressed molecules and therefore has a pole at zero frequency. The strength of this pole is of great interest to us, as we will see in a moment.

The behavior of the propagator for small $\mathbf{k}$ and ω can be studied by expanding around this point. We have

$$
\begin{aligned}
\hbar\Sigma_{11}(\mathbf{k}, z) = & \hbar\Sigma_{11}^{(0,0)} + \Sigma_{11}^{(0,1)} z + \frac{1}{2}\Sigma_{11}^{(0,2)} z^2 + \\
& \Sigma_{11}^{(1,0)} \epsilon(\mathbf{k}) + \dots \\
\hbar\Sigma_{12}(\mathbf{k}, z) = & \hbar\Sigma_{12}^{(0,0)} + \frac{1}{2}\Sigma_{12}^{(0,2)} z^2 + \\
& \Sigma_{12}^{(1,0)} \epsilon(\mathbf{k}) + \dots,
\end{aligned} \tag{39}
$$

where the following definitions have been used

$$
\begin{aligned}
\hbar\Sigma_{11}^{(0,0)} &= \hbar\Sigma_{11}(\mathbf{0}, 0) \\
\hbar\Sigma_{12}^{(0,0)} &= \hbar\Sigma_{12}(\mathbf{0}, 0) \\
\hbar\Sigma_{11}^{(0,1)} &= \left. \frac{\partial}{\partial z} \hbar\Sigma_{11}(\mathbf{k}, z) \right|_{\mathbf{k}=\mathbf{0}, z=0} \\
\hbar\Sigma_{11}^{(0,2)} &= \left. \frac{\partial^2}{\partial z^2} \hbar\Sigma_{11}(\mathbf{k}, z) \right|_{\mathbf{k}=\mathbf{0}, z=0} \\
\hbar\Sigma_{11}^{(1,0)} &= \left. \frac{\partial}{\partial \epsilon(\mathbf{k})} \hbar\Sigma_{11}(\mathbf{k}, z) \right|_{\mathbf{k}=\mathbf{0}, z=0} \\
\hbar\Sigma_{12}^{(1,0)} &= \left. \frac{\partial}{\partial \epsilon(\mathbf{k})} \hbar\Sigma_{12}(\mathbf{k}, z) \right|_{\mathbf{k}=\mathbf{0}, z=0} \\
\hbar\Sigma_{12}^{(0,2)} &= \left. \frac{\partial^2}{\partial z^2} \hbar\Sigma_{12}(\mathbf{k}, z) \right|_{\mathbf{k}=\mathbf{0}, z=0}.
\end{aligned} \tag{40}
$$

We can find analytic expressions for all of these coefficients using Eq. (31).

Now we introduce the spectral function, by Wick-rotating the molecular propagator to real energies, i.e., $G_{\mathrm{m},11}(\mathbf{k}, i\omega) \rightarrow G_{\mathrm{m},11}(\mathbf{k}, \omega^+)$. The imaginary part of this expression gives the spectral function of the bare molecules. This spectral function gives us the wave-function overlap between a bare molecule and the two-atom elementary excitation of our many-body system. For comparison, in the limit of two-body physics, the spectral function can be defined in a similar way. It is given by

$$
\begin{aligned}
&\rho_{\mathrm{m}}(\mathbf{k}, \omega) \\
&= -\frac{1}{\pi} \mathrm{Im}\left[\frac{1}{\hbar\omega^+ - \epsilon(\mathbf{k})/2 - \delta - \hbar\Sigma_{\mathrm{m}}(\hbar\omega^+ - \epsilon(\mathbf{k})/2)} \right],
\end{aligned} \tag{41}
$$

with the self-energy given in Eq. (7). For negative detuning, this spectral function contains a delta peak at negative frequencies, corresponding to the dressed molecular state, and a tail for positive frequencies associated with the two-body scattering states. As the delta peak describes the overlap between the dressed and molecular state, its strength is exactly equal to Z.

In the many-body case, the situation is similar. At zero momentum, the delta peak lies at zero energy, because it is the probability of creating a dressed molecule in the Bose-Einstein condensate. Its strength is equal to the

sought-after factor Z. We derive analytically that

$$\rho_{\mathrm{m}}(\mathbf{k}, \omega) \equiv -\frac{1}{\hbar\pi}\mathrm{Im}\left[G_{11}(\mathbf{k}, \omega^+)\right] \simeq$$
$$+ \left(\frac{1 - \hbar\Sigma_{11}^{(0,1)}}{2\alpha^2} + \frac{|\hbar\Sigma_{12}^{(0,0)}|^{1/2}}{2\alpha\sqrt{\epsilon(\mathbf{k})}}\right)\delta\left(\hbar\omega - \hbar c k\right)$$
$$+ \left(\frac{1 - \hbar\Sigma_{11}^{(0,1)}}{2\alpha^2} - \frac{|\hbar\Sigma_{12}^{(0,0)}|^{1/2}}{2\alpha\sqrt{\epsilon(\mathbf{k})}}\right)\delta\left(\hbar\omega + \hbar c k\right), \quad (42)$$

with $\alpha^2 = (1 - \hbar\Sigma_{11}^{(0,1)})^2 + |\hbar\Sigma_{12}^{(0)}|(\hbar\Sigma_{12}^{(0,2)} - \hbar\Sigma_{11}^{(0,2)})$. The speed of sound is given by

$$c = \left[\frac{1 + 2\hbar\Sigma_{11}^{(1,0)} - 2\hbar\Sigma_{12}^{(1,0)}}{2m\left[\hbar\Sigma_{12}^{(0,2)} - \hbar\Sigma_{11}^{(0,2)} + \left(1 - \hbar\Sigma_{11}^{(0,1)}\right)^2/\hbar\Sigma_{12}^{(0)}\right]}\right]^{1/2}.$$

$$(43)$$

This shows that our theory has reduced to a renormalized Bogoliubov-theory for the bare molecules. The delta peak at positive energy corresponds to a particle-like excitation, and its strength is equal to the Bogoliubov amplitude $Z|u_{\mathrm{m}}(\mathbf{k})|^2$. The delta peak at negative-energy corresponds to a hole-like excitation and has strength $Z|v_{\mathrm{m}}(\mathbf{k})|^2$. Both of these are renormalized by an overall factor Z, but from their separate expressions this is not immediately clear. However, as mentioned before, we expect the combined effect of the two delta peaks at zero momentum to result in a single delta peak in the spectral function with a strength Z. From the expression in Eq. (42) this is found to be the case, and the factor Z is found to be equal to

$$Z = \frac{1 - \Sigma_{11}^{(0,1)}}{(1 - \Sigma_{11}^{(0,1)})^2 + |\hbar\Sigma_{12}^{(0)}|(\Sigma_{12}^{(0,2)} - \Sigma_{11}^{(0,2)})}. \quad (44)$$

IV. BROAD RESONANCES

In the case of a broad resonance, such as the one at 834 G for ^{6}Li, both the molecular density and Z become very small towards the unitarity limit $\delta = 0$. We will discuss the physics of the system using two figures that summarize the main results of our calculations.

In Fig. 7, the spectral function for the bare molecules is given for the BEC-side and the BCS-side of the resonance. The top shows that the BEC-limit shows a structure that resembles the two-body limit. The delta peak is the bare molecular condensate that by definition exists at zero frequency. The continuum of atomic scattering states causes a long tail on the right side of the figure. The distance between these two features is well approximated by the two-body bound state energy $\epsilon_{\mathrm{m}}(\delta)$. The relevant energy scale in this limit is much bigger than the Fermi energy, due to the extreme broadness of the resonance, which is the reason that two-body physics works so well.
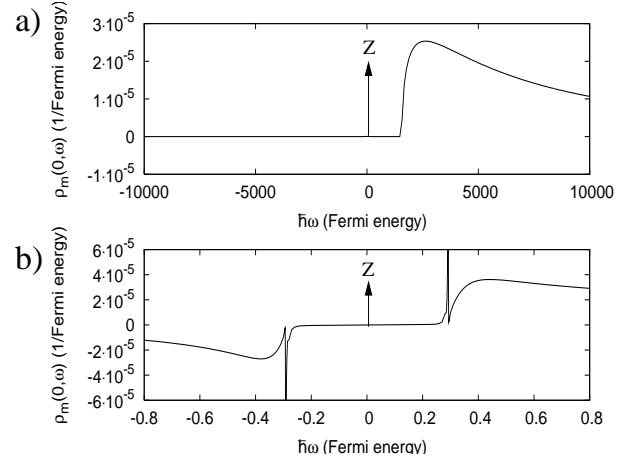

FIG. 7: Spectral functions of the bare ^{6}Li$_2$ molecules with zero momentum a) in the BEC limit at 571 Gauss and b) in the BCS limit at 892 Gauss of the crossover occurring near the broad Feshbach resonance of ^{6}Li at 834 Gauss. The Fermi energy of the gas is 380 nK.

In the bottom half of the same figure we present the spectral density in the BCS-limit that shows completely different physics. Again, the bare molecular condensate is at zero frequency, which is now also the position of twice the Fermi surface, and the two-quasiparticle continuum shows up as particle excitations on the right, and hole excitations on the left. There are no fermionic excitations within 2Δ of twice the chemical potential, as is expected from BCS theory. Left and right we see also the peaks that are expected from RPA theory and physically correspond to the long-lived modes associated with the fluctuations in the magnitude of the BCS gap Δ. A slight curving at these ends anticipates these peaks, which is due to the momentum dependence of the coupling constant g.

In Fig. 8 we then show with the solid line the closed-channel fraction Z as a function of magnetic field. This is an improved version of the figure in Ref. [28], which contained a numerical error in the determination of Z. A comparison is made to the experimental data of Partridge et al. [10]. For reference, the bare molecular condensate density fraction is also plotted. These quantities are not identical and their ratio diverges as δ in the BCS-limit, as we will show later on. The inverse of this ratio is equal to the condensate fraction of dressed molecules, and it is plotted in the inset. Fluctuations become very important on the positive side of the Feshbach resonance, and their contribution to the total density becomes of the same order as the condensate density.

In Fig. 9 we see the behavior of the chemical potential as a function of the magnetic field. For low magnetic fields, the chemical potential is well approximated by half the binding energy of the two-body bound pair $\epsilon_{\mathrm{m}}(\delta)$. This corresponds well to our picture of having a pure Bose-Einstein condensate of dressed molecules in

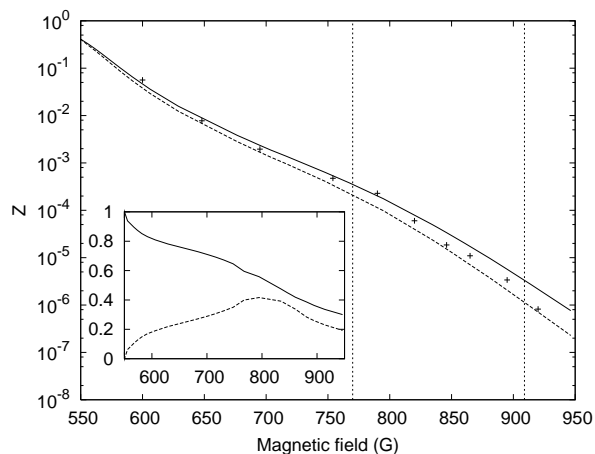FIG. 8: The solid curve shows the probability Z for ^{6}Li. The data points are from the experiment of Partridge et al. [10]. The dashed curve shows for reference the fraction $2Zn_{mc}/n$ as a function of magnetic field. The Fermi energy $\hbar^2 k_F^2/2m$ of the gas is 380 nK. In the inset the solid line shows the Bose-Einstein condensate fraction of dressed molecules $2n_{mc}/n$ and the dashed line the contribution of the fluctuations to the total atomic density. The vertical lines indicate the magnetic fields where $k_F|a_{res}| = 1$.
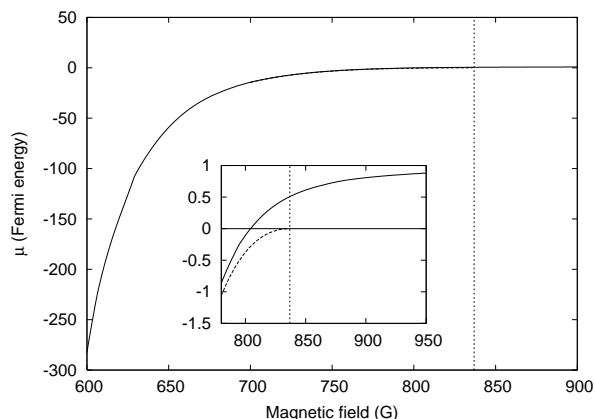
FIG. 9: Chemical potential as a function of magnetic field for ^{6}Li and for the same parameters as in Fig. 8. At unitarity, we find $\mu \simeq 0.51\epsilon_F$. The dashed line is given by $\epsilon_m(\delta)/2$, where $\epsilon_m(\delta)$ is the energy of the dressed molecular state in two-body physics.

this limit. At high magnetic field, the chemical potential saturates and approaches the Fermi energy, as is expected for a fermionic gas. At zero detuning, we have that $\mu \simeq 0.51\epsilon_F$, which is commonly written as $(1+\beta)\epsilon_F$. The result of $\beta \simeq -0.49$ can then be compared to the Monte-Carlo result of $\beta \simeq -0.58$ [37, 38].

The speed of sound, given in Fig. 10, has an interesting behavior, due to the interplay of the resonance, the background scattering, and the dependence on the magnetic field of the different parameters. Apart from
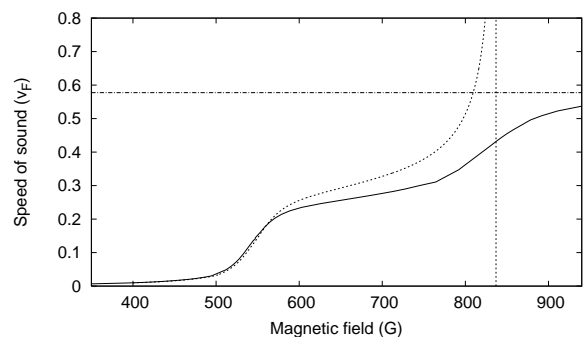

FIG. 10: Speed of sound in the case of ^{6}Li and for the same parameters as in Fig. 8. At unitarity, we find $c \simeq 0.43v_F$. The dashed line is the BEC-limit derived from Eq. (49) using Eqs. (46), (47), and (50). The dash-dotted line is the speed of sound $v_F/\sqrt{3}$ of the Anderson-Bogoliubov mode.

the crossover near resonance, we see around a magnetic field of 550 G, another crossover taking place from the resonant-scattering dominated regime to the background-scattering dominated regime. In the extreme BEC-limit, the sound velocity goes to zero, as the gas approaches the limit of an ideal, noninteracting gas of molecules. On the right it approaches the BCS-like limit of the Anderson-Bogoliubov mode. In the unitarity limit, we find $c \simeq 0.43v_F$. This sound velocity can be compared to previous work [39] where a unitarity value of $c \simeq 0.37v_F$ was found. One of the important reasons for this difference is the inclusion of background scattering effects in our approach.

V. NARROW RESONANCES

We now consider a much narrower resonance, in the absence of background scattering. From an experimental viewpoint, this resonance with $\eta^2 = \epsilon_F$, where ϵ_F is the Fermi energy, is an extremely narrow one, but from a theoretical point of view it is intermediate.

Fig. 11 shows the closed-channel component Z, and the bare molecular condensate density in this case. Again, the difference between Z and the bare condensate fraction is clearly visible. What is interesting here, is that the crossover takes place at a somewhat higher detuning. At zero detuning we still have a large fraction of Bose-Einstein condensed dressed molecules, as they are stabilized by the Fermi-sea, which blocks the dissociation of the condensed molecules. This shift is also observable in Fig. 12, where the chemical potential is plotted as a function of detuning. The chemical potential follows to a large extent the energy level of the bare molecule through the resonance, and only distinctly saturates at positive detuning. At resonance, we now find a lower value of $\mu \simeq 0.17\epsilon_F$. This shows that universality is lost for narrower resonances.

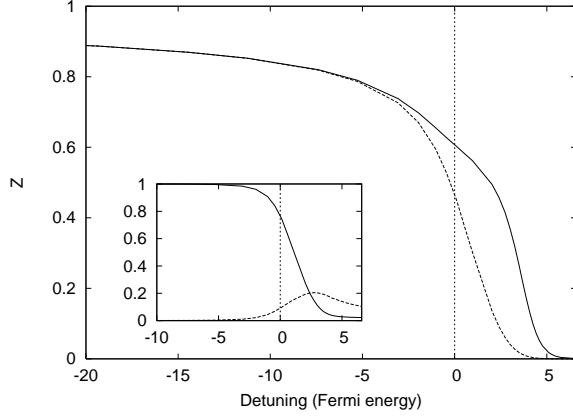The speed of sound, shown in Fig. 13, has a fairly

FIG. 11: The solid curve shows the probability Z for a narrow resonance in the absence of background interactions. The dashed curve shows the fraction $2Zn_{\mathrm{mc}}/n$ as a function of magnetic field. In the inset the solid line shows the Bose-Einstein condensate fraction of dressed molecules $2n_{\mathrm{mc}}/n$ and the dashed line the contribution of the fluctuations to the total atomic density. The vertical line shows the position of the resonance.
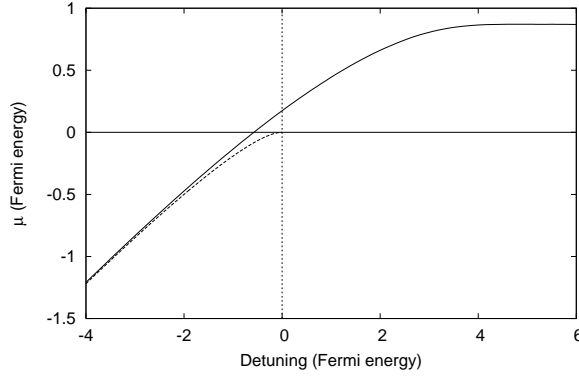

FIG. 12: Chemical potential as function of detuning for a narrow resonance ($\eta^2 = \epsilon_{\mathrm{F}}$). At unitarity, we find $\mu \simeq 0.17\epsilon_F$. The dashed line is given by $\epsilon_{\mathrm{m}}(\delta)/2$, where $\epsilon_{\mathrm{m}}(\delta)$ is the energy of the dressed molecular state in two-body physics.

FIG. 13: Speed of sound in the case of a narrow resonance ($\eta^2 = \epsilon_{\mathrm{F}}$). The dashed curve shows the BEC-limit for a narrow resonance given in Eq. (54). The dash-dotted line is the speed of sound $v_{\mathrm{F}}/\sqrt{3}$ of the Anderson-Bogoliubov mode.

shown in Fig. 14.

FIG. 14: Logarithmic plot of the coefficients in the Bogoliubov Hamiltonian. The coefficients are defined in Eqs. (40). The term that dominates on the BEC-side is a first-order derivative in energy ($\Sigma_{11}^{(0,1)}$), on the BCS-side it is a second-order derivative in energy ($\Sigma_{11}^{(0,2)}$).

straightforward crossover behavior, mainly due to the absence of background scattering. Again we retrieve the Anderson-Bogoliubov mode on the right, and a vanishing speed of sound on the left.

VI. VARIOUS LIMITS OF THE THEORY

In this section we study the three notable limits of the crossover: the BEC-limit, the BCS-limit and the unitarity limit in more detail. Focusing on the microscopic physics and the long-wavelength limit, the crossover can be studied by looking at the behavior of the self-energies for small energies. The various coefficients of interest are
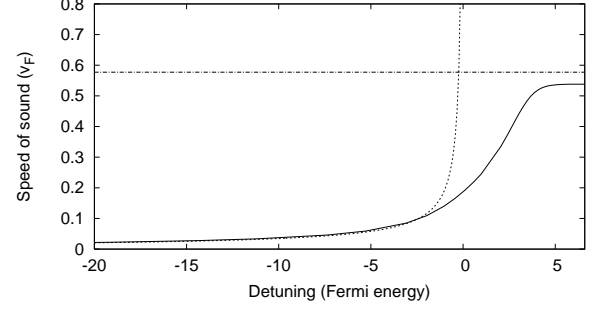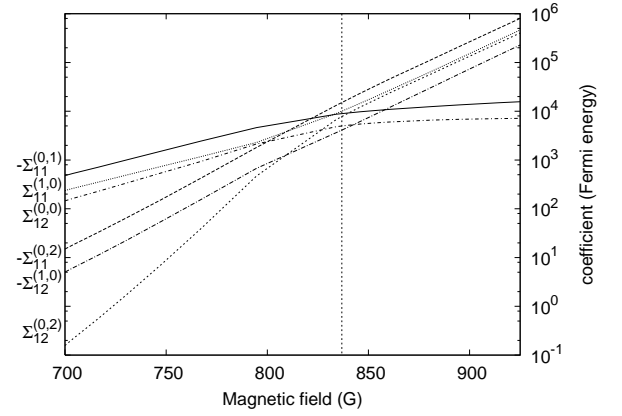
A. BEC-limit

In the BEC-limit, we expect to retrieve the results of two-body physics. The reason for this is that, as a function of the detuning, the chemical potential quickly becomes very negative, eliminating the effects of the Fermi sea. The diagonal terms in the many-body molecular self-energy reduce to the two-body self-energies, and the off-diagonal self-energies become less important. We define the BEC-limit by $|\Delta| \ll |\mu|$. To leading order we

derive from Eq. (31)

$$\hbar\Sigma_{11}(z,\mathbf{k}) = \frac{\eta\sqrt{-z+\epsilon(\mathbf{k})/2 - 2\mu}}{1 + \frac{\sqrt{m}|a_{\mathrm{bg}}|}{\hbar}\sqrt{-z+\epsilon(\mathbf{k})/2 - 2\mu}} \qquad (45)$$

in agreement with Eq. (7). Furthermore, we wish to derive the expression for Z given in Eq. (15). This follows directly from our general Eq. (44) for Z as Σ_{12} is small compared to the diagonal entry Σ_{11}. Thus

$$Z = \frac{1}{1 - \Sigma_{11}^{(0,1)}} = \left(1 + \frac{\eta}{2\sqrt{-2\mu}(1 + \frac{\sqrt{m}|a_{\mathrm{bg}}|}{\hbar}\sqrt{-2\mu})^2}\right)^{-1} \qquad (46)$$

in agreement with Eq. (15). In the BEC limit the fluctuation terms in the equation of state can be neglected. This then suggests that we have only a Bose-Einstein condensate of dressed molecules, and nothing else. Our bare molecules are contained in the term $2\Delta^2/g^2$, the density of bare atoms is given by the term $\mathrm{Tr}[G_a\sigma_3]$. Indeed, defining the density of Bose-Einstein condensed dressed molecules as $n_{\mathrm{mc}} = n/2$, where n is the total density, these terms and the expression for Z reduce to

$$2\Delta^2/g^2 = 2Zn_{\mathrm{mc}}, \qquad (47)$$
$$\mathrm{Tr}[G_a\sigma_3] = 2(1-Z)n_{\mathrm{mc}}. \qquad (48)$$

This is illustrative for the fact that the dressed molecules can be split in a molecular component with contribution Z, and an atomic component with contribution $1 - Z$.

The correct BEC limit for the speed of sound is slightly more involved, as it is not a result of two-body physics. It explicitly depends on the off-diagonal terms in the self-energy as we show next. We can make a straightforward simplification by again using Δ as our small parameter. Furthermore we use the fact that $\Sigma_{11}^{(0,1)} = -2\Sigma_{11}^{(1,0)}$ in this limit. The general expression for the speed of sound is then

$$c = \left[\frac{\hbar\Sigma_{12}^{(0)}}{2m\left(1 - \Sigma_{11}^{(0,1)}\right)}\right]^{1/2}. \qquad (49)$$

Depending on the background scattering length, the width of the resonance, and the density, the system can enter different regimes. Expanding in the parameter $\Delta/|\mu|$, the off-diagonal term reduces to

$$\hbar\Sigma_{12}^{(0)} = \frac{\Delta^2\eta}{16(-\mu)^{3/2}(1+2\mu/E_{\mathrm{bg}})^4}\left(32\left(\frac{-\mu}{E_{\mathrm{bg}}}\right)^{5/2} - 60\sqrt{2}\left(\frac{\mu}{E_{\mathrm{bg}}}\right)^2 + 80\left(\frac{-\mu}{E_{\mathrm{bg}}}\right)^{3/2} + 20\sqrt{2}\frac{\mu}{E_{\mathrm{bg}}} + \sqrt{2}\right), \qquad (50)$$

where $E_{\mathrm{bg}} = \hbar^2/ma_{\mathrm{bg}}^2$. The gap is fundamentally a many-body property, but it can be related to the two-body Z and the density through Eq. (47). One possible

regime is $|\mu| \ll E_{\mathrm{bg}}$, where the background scattering is small, while being sufficiently close to resonance such that $|\delta| \ll \eta^2$, yet sufficiently far to be in the BEC-limit. In that regime the resonant scattering determines the speed of sound, and we find the simple expression

$$c = \hbar\sqrt{2\pi a_{\mathrm{res}}n_{\mathrm{mc}}}/m, \qquad (51)$$

where $a_{\mathrm{res}} = \hbar\eta/\delta\sqrt{m} = \hbar\eta/\Delta\mu(B - B_0)\sqrt{m}$ is the resonant scattering length, and n_{mc} is the Bose-Einstein condensate density of dressed molecules. This can be cast in the more familiar result

$$c = \hbar\sqrt{4\pi a_{\mathrm{m}}n_{\mathrm{mc}}}/m_{\mathrm{m}}, \qquad (52)$$

using the relevant parameters for molecules $a_{\mathrm{m}} = 2a_{\mathrm{res}}$ [40] and $m_{\mathrm{m}} = 2m$. This is precisely the Bogoliubov speed of sound [41]. Note that the Bose-Einstein condensate density of dressed molecules shows up in the expression for the speed of sound, further strengthening the case that the dressed molecules are the relevant physical entities in this system. In the case of ^{6}Li, at densities that are typical for experiment, this regime is however not well separated from other regimes, due to the extremely large background scattering.

Before we move on to the background-scattering dominated regime, we compare our results to single-channel theory. In this case there is only a single parameter, the total atomic scattering length $a = a_{\mathrm{res}} + a_{\mathrm{bg}}$. Assuming the validity of Eq. (52), the molecular scattering length can be derived from the speed of sound, and expressed in terms of the total atomic scattering length a. This is shown in Fig. 15. The expected one-loop single-channel result $a_m = 2a$ is given by the dashed line and can basically never be considered as a good approximation to the one-loop result obtained from our two-channel theory. We expect the same to be true of the exact single-channel result.
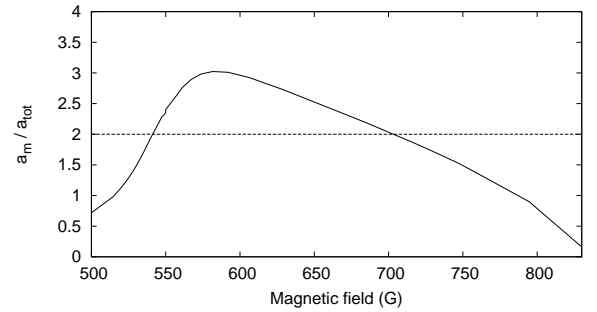

FIG. 15: Ratio of the molecular and total atomic scattering length as a function of magnetic field.

When the background scattering gives a significant contribution, and $|\mu| \simeq E_{\mathrm{bg}}$, which for ^{6}Li at the densities of interest happens roughly around a magnetic field of 650 G, it has a strong effect on the speed of sound.

Taking it into account using Eq. (50), and relating the speed of sound to the two-body Z as described above, we get the result that is drawn by the dashed line in Fig. 10. We can conclude that the speed of sound is not so well approximated with two-body physics as the closed-channel component Z. This is maybe to be expected as the speed of sound is really a many-body property of the gas.

In the extreme BEC-limit, the speed of sound vanishes as

$$c = \left(\frac{\eta g^2 n E_{\mathrm{bg}}^{3/2}}{2[-\epsilon_{\mathrm{m}}(\delta)]^3} \right)^{1/2}, \tag{53}$$

where $\epsilon_{\mathrm{m}}(\delta)$ is the energy of the exact bound molecular state taken from Eq. (8). In this way the theory is completely reduced to two-body physics, where there indeed exists no sound. Of course, the vanishing of the speed of sound in the extreme BEC limit is a result of the fact that we neglected the background scattering between molecules. If this is effectively repulsive, it will ultimately stabilize the molecular condensate and result in a nonzero speed of sound. Finally, in theory we can also be far away from resonance, and in a regime where the effect of the atomic background scattering is small. In this case the speed of sound reduces to

$$c = \left(\frac{\eta g^2 n}{8(-\delta)^{3/2}} \right)^{1/2}. \tag{54}$$

This solution is shown by the dashed line in Fig. 13.

B. BCS-limit

For large positive detuning, the system strongly resembles that of a normal BCS superfluid. The density of bare molecules becomes exponentially small, and the properties of the system depend mainly on the gap parameter Δ, which is also decreasing exponentially. Moreover, the chemical potential tends to the Fermi energy.

Again, we can study the system by looking at the action for long wavelengths. We find explicitly,

$$\begin{aligned}
\hbar\Sigma_{11}^{(0)} &\simeq \frac{2\sqrt{2}}{\pi}\eta\frac{\sqrt{\epsilon_{\mathrm{F}}}}{1+2\epsilon_{\mathrm{F}}/E_{\mathrm{bg}}} \log(\Delta/\epsilon_{\mathrm{F}}), \\
\hbar\Sigma_{12}^{(0)} &\simeq \frac{\sqrt{2}}{\pi}\eta\frac{\sqrt{\epsilon_{\mathrm{F}}}}{1+2\epsilon_{\mathrm{F}}/E_{\mathrm{bg}}}, \\
\hbar\Sigma_{11}^{(0,1)} &\simeq \frac{2\sqrt{2}}{\pi}\frac{\eta}{\sqrt{\epsilon_{\mathrm{F}}}}\frac{1-2\epsilon_{\mathrm{F}}/E_{\mathrm{bg}}}{4(1+2\epsilon_{\mathrm{F}}/E_{\mathrm{bg}})} \log(\Delta/\epsilon_{\mathrm{F}}), \\
\hbar\Sigma_{11}^{(0,2)} &\simeq -2\sqrt{2\epsilon_{\mathrm{F}}}\eta/3\pi\Delta^2 \\
\hbar\Sigma_{12}^{(0,2)} &\simeq \sqrt{2\epsilon_{\mathrm{F}}}\eta/3\pi\Delta^2 \\
\hbar\Sigma_{11}^{(1,0)} &\simeq 4\sqrt{2}\epsilon_{\mathrm{F}}^{3/2}\eta/9\pi\Delta^2 \\
\hbar\Sigma_{12}^{(1,0)} &\simeq -2\sqrt{2}\epsilon_{\mathrm{F}}^{3/2}\eta/9\pi\Delta^2,
\end{aligned} \tag{55}$$

where ϵ_{F} is the Fermi energy. We see that the coefficients $\Sigma_{11}^{(0,2)}$, $\Sigma_{12}^{(0,2)}$, $\Sigma_{11}^{(1,0)}$ and $\Sigma_{12}^{(1,0)}$ diverge most strongly for

small Δ. We can use Eq. (43) to find the speed of sound in this limit and we obtain

$$c = \frac{v_{\mathrm{F}}}{\sqrt{3}}, \tag{56}$$

where v_{F} is the Fermi velocity $\hbar k_{\mathrm{F}}/m$. This coincides with the speed of sound of the Anderson-Bogoliubov mode [42, 43, 44]. A more illustrative way of deriving this result is to determine the eigenvalues of the propagator in the long-wavelength limit. The leading terms are the ones mentioned above, leading to

$$S_{\mathrm{m}}[\psi_{\mathrm{m}}^*, \psi_{\mathrm{m}}] \simeq \frac{\sqrt{2\epsilon_{\mathrm{F}}}\eta}{36\pi\Delta^2} \sum_{\mathbf{k},n} [\psi_{\mathrm{m}}^*, \psi_{\mathrm{m}}] \tag{57}$$

$$\times \begin{bmatrix} 6(\hbar\omega)^2 + 8\epsilon_{\mathbf{k}}\epsilon_{\mathrm{F}} & -3(\hbar\omega)^2 - 4\epsilon_{\mathbf{k}}\epsilon_{\mathrm{F}} \\ -3(\hbar\omega)^2 - 4\epsilon_{\mathbf{k}}\epsilon_{\mathrm{F}} & 6(\hbar\omega)^2 + 8\epsilon_{\mathbf{k}}\epsilon_{\mathrm{F}} \end{bmatrix} \begin{bmatrix} \psi_{\mathrm{m}} \\ \psi_{\mathrm{m}}^* \end{bmatrix}.$$

This action can be diagonalized by introducing amplitude and phase fluctuations. Keeping in mind that ψ_{m} are the fluctuations of the molecular field, we define $\psi_{\mathrm{m}} = \rho/g + i\Delta\theta/g$ and $\psi_{\mathrm{m}}^* = \rho/g - i\Delta\theta/g$, to obtain

$$\begin{aligned}
S_{\mathrm{m}}[\rho, \theta] &\simeq \frac{\sqrt{2\epsilon_{\mathrm{F}}}\eta}{18\pi g^2\Delta^2} \sum_{\mathbf{k},n} [\rho^*, \Delta\theta^*] \times \\
&\begin{bmatrix} 3(\hbar\omega)^2 + 4\epsilon(\mathbf{k})\epsilon_{\mathrm{F}} & 0 \\ 0 & 9(\hbar\omega)^2 + 12\epsilon(\mathbf{k})\epsilon_{\mathrm{F}} \end{bmatrix} \begin{bmatrix} \rho \\ \Delta\theta \end{bmatrix} \\
&= \frac{N(0)}{36} \sum_{\mathbf{k},n} \left(\frac{|\rho(\mathbf{k}, i\omega_n)|^2}{\Delta^2} + 3|\theta(\mathbf{k}, i\omega_n)|^2 \right) \\
&\times \left(3(\hbar\omega)^2 + 4\epsilon(\mathbf{k})\epsilon_{\mathrm{F}} \right),
\end{aligned} \tag{58}$$

in agreement with Ref. [45]. Here $N(0)$ is the density of states of a single spin state at the Fermi surface. We expect that the non-leading terms in Δ lead to a mass term of order Δ^2 for the amplitude fluctuations. The result in Eq. (56) can be immediately derived from the phase fluctuation part.

The closed-channel component in the BCS-limit is

$$Z = \frac{\pi(1 - 2\epsilon_{\mathrm{F}}/E_{\mathrm{bg}})}{2\sqrt{2}\eta\epsilon_{\mathrm{F}}^{3/2}} \Delta^2 \log\left(\epsilon_{\mathrm{F}}/\Delta\right). \tag{59}$$

It is important to notice that in this BCS limit, Z and the density contribution of the Bose-Einstein condensate of bare molecules $2\Delta^2/g^2$ have an entirely different behavior as a function of detuning. From the gap equation it can be derived that the gap vanishes exponentially,

$$\Delta \propto \epsilon_{\mathrm{F}} \exp\left\{ -\frac{\pi(1 + 2\epsilon_{\mathrm{F}}/E_{\mathrm{bg}})}{2\eta\sqrt{2\epsilon_{\mathrm{F}}}}\delta \right\}, \tag{60}$$

thus the ratio between Z and Δ^2 diverges linearly with the detuning. This shows that these are different entities with different physical meanings.

C.   Unitarity limit

For $\delta = 0$ we can make a rough estimate of Z, that gives a simple physical reason for why Z is small for broad Feshbach resonances. As can be seen in Fig. 7, the most notable result of the many-body theory is the gap around the Fermi surface. In contrast to two-body physics, where Z goes to zero at resonance, the many-body physics stabilizes the pairs, much like Cooper-pairs. For broad resonances, the spectral function has a long tail at high energies, which is not affected by many-body physics because it lies far above the Fermi energy. Using the fact that the spectral function is normalized to one, we can thus approximate the spectral weight in the delta function by integrating the two-body spectral function over an energy interval of twice the gap.

$$Z \simeq \frac{1}{\pi} \int_0^{2\Delta} \frac{\sqrt{z}\eta}{z^2 + \eta^2 z} dz \simeq \frac{2\sqrt{2\Delta}}{\pi\eta} \qquad (61)$$

From our calculations, the gap at unitarity is equal to $0.46\epsilon_{\mathrm{F}}$, which is quite close to the Monte-Carlo result of $\Delta \simeq 0.50\epsilon_{\mathrm{F}}$ [38]. Substituting this in Eq. (61) results in an approximate value for Z of $3.5 \cdot 10^{-5}$, which is only about 20% lower than the result of our Bogoliubov theory.

VII.   CONCLUSIONS

The BEC-BCS crossover near a Feshbach resonance is very rich in physics. We have presented a theory that rigorously incorporates the two-body Feshbach physics and, due to the inclusion of fluctuations, allows for an accurate study of the full crossover problem, both for broad and narrow resonances. We calculated the probability Z, that is crucial in understanding the microscopic physics of the crossover, and studied the molecular spectral function and the spectrum of collective modes throughout the BEC-BCS crossover. Where possible, we have compared our theory with experiment and have found a satisfying agreement, even in the unitarity limit where the interactions are very strong.

[1] M.H. Anderson, J. Ensher, M. Matthews, E. A. Cornell, and C. E. Wieman, Science **269**, 198 (1995).
[2] K. B. Davis, M. O. Mewes, M. R. Andrews, N. J. van Druten, D. S. Durfee, D. M. Kurn, and W. Ketterle, Phys. Rev. Lett. **75**, 3969 (1995).
[3] C. C. Bradley, C. A. Sackett, J. J. Tollett, and R. G. Hulet, Phys. Rev. Lett. **75**, 1687 (1995).
[4] B. DeMarco and D. S. Jin, Science **285**, 1703 (1999).
[5] C. A. Regal, M. Greiner, and D. S. Jin, Phys. Rev. Lett. **92**, 040403 (2004).
[6] M. W. Zwierlein, C. A. Stan, C. H. Schunck, S. M. F. Raupach, A. J. Kerman, and W. Ketterle, Phys. Rev. Lett. **92**, 120403 (2004).
[7] J. Kinast, S. L. Hemmer, M. E. Gehm, A. Turlapov, and J. E. Thomas, Phys. Rev. Lett. **92**, 150402 (2004); Science **307**, 1296 (2005).
[8] M. Bartenstein, A. Altmeyer, S. Riedl, S. Jochim, C. Chin, J. H. Denschlag, and R. Grimm, Phys. Rev. Lett. **92**, 120401 (2004); Phys. Rev. Lett. **92**, 203201 (2004).
[9] T. Bourdel, L. Khaykovich, J. Cubizolles, J. Zhang, F. Chevy, M. Teichmann, L. Tarruell, S. J. J. M. F. Kokkelmans, and C. Salomon, Phys. Rev. Lett. **93**, 050401 (2004).
[10] G. B. Partridge, K. E. Strecker, R. I. Kamar, M. W. Jack, and R. G. Hulet, Phys. Rev. Lett. **95**, 020404 (2005).
[11] H. Feshbach, Ann. Phys. **5**, 357 (1958); Ann. Phys. **19**, 287 (1962).
[12] W. C. Stwalley, Phys. Rev. Lett. **37**, 1628 (1976).
[13] E. Tiesinga, B. J. Verhaar, and H. T. C. Stoof, Phys. Rev. A **47**, 4114 (1993).
[14] D. M. Eagles, Phys. Rev. **186**, 456 (1969).
[15] A. J. Leggett, in *Modern Trends in the Theory of Condensed Matter* (Springer-Verlag, Berlin, 1980), p. 13.
[16] P. Nozieres and S. Schmitt-Rink, J. Low Temp. Phys. **59**, 195 (1985).
[17] G. M. Falco and H. T. C. Stoof, Phys. Rev. Lett. **92**, 130401 (2004).
[18] A. Perali, P. Pieri, L. Pisani, and G. C. Strinati, Phys. Rev. Lett. **92**, 220404 (2004).
[19] J. Stajic, Q. Chen, and K. Levin, Phys. Rev. Lett. **94**, 060401 (2005).
[20] M. Mackie and J. Piilo, Phys. Rev. Lett. **94**, 060403 (2005).
[21] R. B. Diener and T.-L. Ho, cond-mat/0404517.
[22] Y. Ohashi and A. Griffin, Phys. Rev. A **72**, 013601 (2005).
[23] M. H. Szymanska, K. Goral, T. Köhler, and K. Burnett, Phys. Rev. A **72**, 013610 (2005).
[24] S. Diehl and C. Wetterich, Phys. Rev. A **73**, 033615 (2006).
[25] G. E. Astrakharchik, R. Combescot, X. Leyronas, S. Stringari, Phys. Rev. Lett. **95**, 030404 (2005).
[26] Q. Chen and K. Levin, Phys. Rev. Lett. **95**, 260406 (2005).
[27] J. Javanainen, M. Kostrun, M. Mackie and A. Carmichael, Phys. Rev. Lett. **95**, 110408 (2005).
[28] M. W. J. Romans and H. T. C. Stoof, Phys. Rev. Lett. **95**, 260407 (2005).
[29] For a review see R. A. Duine and H. T. C. Stoof, Phys. Rep. **396**, 115 (2004).
[30] H. Moritz, T. Stöferle, K. Günter, M. Köhl, and T. Esslinger, Phys. Rev. Lett. **94**, 210401 (2005).

[31] N. Nygaard, B. I. Schneider, P. S. Julienne, Phys. Rev. A **73**, 042705 (2006)

[32] S. Jochim, M. Bartenstein, A. Altmeyer, G. Hendl, C. Chin, J. Hecker Denschlag, and R. Grimm, Phys. Rev. Lett. **91**, 240402 (2003).

[33] G. M. Falco and H. T. C. Stoof, Phys. Rev. A **71**, 063614 (2005).

[34] P. D. Drummond, K. V. Kheruntsyan, and H. He, Phys. Rev. Lett. **81**, 3055 (1998).

[35] E. Timmermans, P. Tommasini, H. Hussein, and A. Kerman, Phys. Rep. **315**, 199 (1999).

[36] N. M. Hugenholtz and D. Pines, Phys. Rev. **116**, 489 (1959).

[37] G. E. Astrakharchik, J. Boronat, J. Casulleras, and S. Giorgini, Phys. Rev. Lett. **93**, 200404 (2004).

[38] J. Carlson and S. Reddy, Phys. Rev. Lett. **95**, 060401 (2005).

[39] T. K. Ghosh and K. Machida, Phys. Rev. A **73**, 013613 (2006).

[40] C. A. R. Sá de Melo, Mohit Randeria, and Jan R. Engelbrecht, Phys. Rev. Lett. **71**, 3202 (1993).

[41] N. N. Bogoliubov, J. Phys. USSR **11** 23 (1947).

[42] P.W. Anderson, Phys. Rev. **112**, 1900 (1958).

[43] N.N. Bogoliubov, V.V. Tolmachev and D.V. Shirkov, *A New Method in the Theory of Superconductivity*, Translated from Russian (New York, Consultants Bureau, 1959).

[44] V.M. Galitskii, Sov. Phys. JETP **34 (7)**, 698 (1958).

[45] H. T. C. Stoof, Phys. Rev. B **47**, 7979 (1993).